Palaeogeography, Palaeoclimatology, Palaeoecology

Benthic Foraminiferal Salinity index in marginal-marine environments: a case study from the Holocene Guadalquivir estuary, SW Spain

--Manuscript Draft--

Manuscript Number:	PALAEO-D-20-00166R4
Article Type:	Research Paper
Keywords:	Micropaleontology; Coastal settings; Restriction; Quaternary; Brackish; Europe
Corresponding Author:	José N. Pérez-Asensio CEREGE AIX-EN-PROVENCE, PACA FRANCE
First Author:	José N. Pérez-Asensio
Order of Authors:	José N. Pérez-Asensio
	Antonio Rodríguez-Ramírez
Manuscript Region of Origin:	Europe
Abstract:	Here we developed and validated a new Benthic Foraminiferal Salinity (BFS) index from marginal-marine environments by analysing benthic foraminifera from the Holocene Guadalquivir estuary sediments (SW Spain). This index is formulated utilising only four species: Ammonia tepida and Haynesina germanica with higher tolerance to brackish waters and indicating lower salinity, and Elphidium translucens and Elphidium granosum indicative of greater marine influence and pointing to higher salinity. Thus, the BFS index is calculated easily and rapidly, and therefore it makes it possible to analyse a higher number of samples in less time. The BFS index values from the studied cores enabled the detailed description of subtle changes in the Guadalquivir estuary restriction during the Holocene. For this purpose, three degrees of salinity, depending on marine influence, were defined: higher (BFS index = 0.0-0.4, high marine influence), moderate (BFS index = 0.4-0.7, moderate marine influence), and lower (BFS index = 0.7-1.0, low marine influence). Before 2000 BCE, the estuary was moderately open and well-connected to the Atlantic Ocean. From 2000 BCE, the estuary experienced a greater marine influence, increasing in extension, as a consequence of a sea-level rise and subsidence. Immediately afterwards, it began to experience restriction processes due to southward shoreline progradation related to the growth of littoral spits and sediment supply. From 1400 to 1000 BCE, gradual restriction transformed the open estuary into a semiclosed estuary. A last phase of estuary restriction occurred from 1000 BCE to the present day, leading to the lowest salinity and the highest estuary restriction. Finally, the BFS index was successfully applied in two other marginal-marine environments: a Pleistocene lagoon in northern Italy, and a Pliocene coastal bay in southeastern Spain. The index allowed assessment of the degree of restriction in these different environments, supporting its utility in different regions, environments and timescales.
Suggested Reviewers:	Letizia Di Bella Universita degli Studi di Roma La Sapienza Dipartimento di Scienze della Terra letizia.dibella@uniroma1.it Renowned specialist on benthic foraminiferal paleoecology and paleoenvironmental reconstructions
	Ana Maria Blazquez Universidad Catolica de Valencia San Vicente Martir ana.blazquez@ucv.es Reputed expert on benthic foraminifera from coastal and marginal environments
	Elisabeth Alve Department of Geosciences, University of Oslo elisabeth.alve@geo.uio.no Specialist on benthic foraminiferal paleoecology
	Virginia Alves Martins Universidade do Estado do Rio de Janeiro

	virginia.martins@ua.pt Expert on paleoenvironmental reconstructions based on benthic foraminifera
	Stefano Claudio Vaiani Department of Biological, Geological and Environmental Sciences, University of Bologna stefano.vaiani@unibo.it Expert on benthic foraminifera from coastal environments
Response to Reviewers:	

Benthic Foraminiferal Salinity index in marginal-marine environments: a case study from the Holocene Guadalquivir estuary, SW Spain

José N. Pérez-Asensio[a,*], Antonio Rodríguez-Ramírez[b]

Authors' addresses:

[a] *CEREGE UM34, Aix Marseille Univ, CNRS, IRD, INRAE, Coll France, 13545 Aix-en-Provence, France*

[b] *Departamento de Ciencias de la Tierra, Universidad de Huelva, Campus de Excelencia Internacional de Medio Ambiente, Biodiversidad y Cambio Global, CEI-Cambio, Avenida de las Fuerzas Armada s/n, 21007 Huelva, Spain*

* Corresponding author; E-mail address: perez@cerege.fr (José N. Pérez-Asensio)

Second author; E-mail address: arodri@uhu.es (Antonio Rodríguez-Ramírez)

Abstract

Here we developed and validated a new Benthic Foraminiferal Salinity (BFS) index from marginal-marine environments by analysing benthic foraminifera from the Holocene Guadalquivir estuary sediments (SW Spain). This index is formulated utilising only four species: *Ammonia tepida* and *Haynesina germanica* with higher tolerance to brackish waters and indicating lower salinity, and *Elphidium translucens* and *Elphidium granosum* indicative of greater marine influence and pointing to higher salinity. Thus, the BFS index is calculated easily and rapidly, and therefore it makes it possible to analyse a higher number of samples in less time. The BFS index values from the studied cores enabled the detailed description of subtle changes in the Guadalquivir estuary restriction during the Holocene. For this purpose, three degrees of salinity, depending on marine influence, were defined: higher (BFS index =

0.0-0.4, high marine influence), moderate (BFS index = 0.4-0.7, moderate marine influence), and lower (BFS index = 0.7-1.0, low marine influence). Before 2000 BCE, the estuary was moderately open and well-connected to the Atlantic Ocean. From 2000 BCE, the estuary experienced a greater marine influence, increasing in extension, as a consequence of a sea-level rise and subsidence. Immediately afterwards, it began to experience restriction processes due to southward shoreline progradation related to the growth of littoral spits and sediment supply. From 1400 to 1000 BCE, gradual restriction transformed the open estuary into a semiclosed estuary. A last phase of estuary restriction occurred from 1000 BCE to the present day, leading to the lowest salinity and the highest estuary restriction. Finally, the BFS index was successfully applied in two other marginal-marine environments: a Pleistocene lagoon in northern Italy, and a Pliocene coastal bay in southeastern Spain. The index allowed assessment of the degree of restriction in these different environments, supporting its utility in different regions, environments and timescales.

Keywords: Micropaleontology; Coastal settings; Restriction; Brackish; Quaternary; Europe

1. Introduction

Marginal-marine environments, including estuaries, deltas, fjords, marshes and littoral lagoons, are very sensitive to changes in sea level, tide and wave regime, as well as fluvial dynamics (Chiverrell, 2001; Ybert et al., 2003). These factors play a key role in controlling coastal geomorphological features (spits, dunes, cheniers, marshes, levees, tidal channels), and sedimentary features (sediment supply, sedimentary bodies, sediment infilling), which modify the paleogeography of marginal-marine environments (Gerdes et al., 2003; Durand et al., 2016). Coastal environments occur at the transition between continental fresh waters and

marine normal salinity waters, consequently they are commonly characterised by brackish waters (Rich and Maier, 2015). In coastal environments, the gradual decrease of seawater influence reduces salinity (Guelorget and Perthuisot, 1983, 1992; Debenay, 1995). Thus, marginal-marine environments have lower or higher salinity depending on the lower or higher influence of marine waters, respectively. Salinity is governed by the geomorphological restriction of the coastal environment (i.e., degree of connection to the open sea), which is related to changes in both geomorphological and sedimentary features (Gregoire et al., 2017; Devillers et al., 2019; Haas et al., 2019). Therefore, lower or higher restriction causes higher or lower salinity, respectively.

Benthic foraminifera are widely used for reconstructing paleoenvironmental changes from marginal-marine to deep-sea environments since they are very sensitive to variations in sea level, organic fluxes, oxygen content, salinity and type of substrate (e.g., Alve and Murray, 1999; Jorissen et al., 2007; Di Bella et al., 2008; Martins et al., 2014; Blázquez et al., 2017; Pérez-Asensio et al., 2014, 2017, 2020). In coastal settings, it is well known that benthic foraminiferal distribution and abundance can be influenced by salinity, which is dependent, among other factors, on the geomorphological restriction (Debenay et al., 2006; Barbieri and Vaiani, 2018; Blázquez-Morilla et al., 2019). In fact, benthic foraminifera have been successfully used as proxies of restriction of marginal-marine environments and for developing salinity indices (Debenay, 1995; Hayward et al., 2004; Debenay and Luan, 2006). Previously defined salinity indices (Debenay, 1995; Hayward et al., 2004) are based on complex and time-consuming identification of numerous benthic foraminiferal species, which requires a profound taxonomic knowledge. Hence, it is necessary to create simpler salinity indices based on a low number of species, which would be useful for scientists who are not specialized on benthic foraminiferal taxonomy. Furthermore, identifying fewer species would imply a faster process

for obtaining foraminiferal data, making it possible to analyse more sedimentary records at higher resolution.

The principal objectives of this study were to develop a simple Benthic Foraminiferal Salinity (BFS) index, and to validate it as proxy for different degrees of salinity in marginal-marine environments. For these purposes, we analysed benthic foraminifera from 8 short cores (this study) and two deep cores (Rodríguez-Ramírez et al., 2015), which recovered Holocene sediments from the Guadalquivir estuary (SW Spain) (Figs 1 and 2). The Guadalquivir estuary is an excellent area to assess the performance of our BFS index because its paleogeography, and therefore its connection to the open sea (i.e., marine influence), changed substantially over the Holocene owing to geomorphological and sedimentary processes (Rodríguez-Ramírez et al., 2019). In addition, the applicability of this BFS index was tested in two different environments (lagoon, coastal bay) from other regions (northern Italy, southeastern Spain).

2. Study area: the Guadalquivir estuary

The Guadalquivir estuary (SW Spain) is located in the Gulf of Cadiz (Atlantic Ocean) (Fig. 1). It contains a 180,000 ha freshwater marsh including the Doñana National Park (UNESCOMAB Biosphere Reserve). This estuary has two enclosing spits (Doñana and La Algaida), which are partly covered by active dunes. Both spits protect a wide marsh area behind. This marsh grew without sediment input from the Guadalquivir and convergent rivers because this riverine sediment supply filled in the ancient marine Guadalquivir estuary as finger deltas in a low-energy setting. The growth of the two large littoral spits isolating the estuary and the development of a wide chenier plain favoured this sedimentary process (Rodríguez-Ramírez and Yáñez-Camacho, 2008).

Fluvial regime, tidal inflow, wave action, and drift currents controlled the Guadalquivir estuary hydrodynamics. The Guadalquivir river is the largest river draining SW Spain and the principal source for fluvial sediments in the southwestern Spanish coast. This river has a mean annual discharge of 164 m^3/s, with winter spates that can easily exceed 5000 m^3/s (Vanney, 1970). At the river mouth in the period from 1997 to 2003, the average tidal range was 2 m with a maximal tidal range of 3.86 m (Spanish Ministry of Fomento, 2005). Accordingly, the coastline is mesotidal, semidiurnal.

The wave regime is directly related to the prevailing SW winds, with 22.5% of the days of the year with SW winds (Rodríguez-Ramírez et al., 2003). Overall, the wave regime has medium-to-low energy, with waves normally <0.6 m high (data of Departamento de Clima Marítimo). Atlantic cyclones are frequent during winter and they foster strong SW winds, generating significant erosion in the coastline (Rodríguez-Ramírez et al., 2003). Most of the wave fronts approach obliquely the coastline generating longshore currents that transport sand from the Portuguese coast to Spanish nearshore areas.

3. Methodology

3.1. Lithostratigraphy

We studied the sedimentary sequences and facies from 8 short cores (<3 m): S6, LB, AR, AA, VT, VAc, VAli.2 and VAli.1 (Table 1). The cores were drilled with a 4-cm-diameter Eijkelkamp gouge, an 8-cm-diameter drill, and trenches. We also analysed previously published sedimentary records from two long cores: S7 and S11 (Table 1) (Rodríguez-Ramírez et al., 2015). Grain-size analyses were performed using conventional sieving for fractions >2 mm, and a Malvern Mastersizes 2000 laser diffraction particle analyser for smaller particle

sizes between 2 mm and 2 μm. Shepard's sediment classification (Shepard, 1954) was applied to grain-size results in order to describe sediment texture, including sand, silt and clay fractions.

3.2. Radiocarbon dating

Eight new radiocarbon dates were measured on mollusc shells at the laboratories of Centro Nacional de Aceleradores (Seville, Spain) and Accium BioSciences Accelerator Mass Spectrometry Lab (Seattle, USA) (Table 2, Fig. 2). Other 14 radiocarbon dates from previous studies (Rodríguez-Ramírez et al., 2014, 2015, 2016) were used in this work (Table 2, Fig. 2). Calibration of radiocarbon data was conducted by means of CALIB 7.10 software (Stuiver and Reimer, 1993) and the calibration dataset of Reimer et al. (2013). Uncertainties of the calibrated ages are expressed as 2σ errors. The reservoir effect was corrected using the ΔR values recommended by Soares (2015). This author suggested a ΔR value of −108 ± 31 ^{14}C yr for the late Holocene on the Andalusian coast of the Gulf of Cadiz; excluding the years 4400–4000 ^{14}C yr BP, for which he recommended a ΔR value of +100 ± 100 ^{14}C yr. In the interval from 4000 to 2000 ^{14}C yr BP, lack of data impedes pinpointing the most recent time boundary to which the +100 ± 100 ^{14}C yr ΔR value can be extended. In spite of this problem, we decided to tentatively extend it to the middle year 3000 ^{14}C yr BP.

3.3. Micropaleontology

A total of 45 sediment samples (~50 g) was wet-sieved over a 63 μm mesh and dried in an oven at 40°C. Samples were thoroughly split using a microsplitter so as to obtain sub-samples. Then, theses sub-samples were dry-sieved over a 125 μm mesh, and at least 300 benthic foraminifera were carefully counted and identified to the species level (Loeblich and Tappan, 1987; Milker and Schmiedl, 2012; Pérez-Asensio et al., 2012). Raw counts were

transformed into relative abundances (%). Q-mode principal component analysis (PCA) was carried out on all samples from the short and long cores using the software OriginPro 2020. All species were included in the analysis. The PCA allowed to establish benthic foraminiferal assemblages and to infer environmental factors controlling these assemblages (Parker and Arnold, 1999; Milker et al., 2009) (Table 3, Fig. 3).

In this study, we developed a new Benthic Foraminiferal Salinity (BFS) index for assessing the salinity changes in marginal-marine environments (e.g., estuaries, lagoons, marshes). This BFS index is based on the distribution of some of the dominant benthic foraminiferal species found in the Holocene Guadalquivir estuary sediments (see discussion section 5.2).

4. Results

4.1. Lithostratigraphy and chronology of the deep cores: S7 and S11

The sedimentary sequence and chronology of deep cores S7 and S11 are described in detail in prior studies (Jiménez-Moreno et al., 2015; Rodríguez-Ramírez et al., 2015).

The core S11 is 18 m long and its lower part (18 to 12.5 m) consists of a Pleistocene marsh sequence of mostly greyish ochre clayey silts (Fig. 2). From 12.5 m to the top, the Holocene sequence is dominated by grey-greenish clayey silts, with three intercalated sandy layers at around 12, 9, and 7 m (Fig. 2). These sandy layers have been interpreted as Extreme Wave Events (EWEs) (Rodríguez-Ramírez et al., 2015) occurring at ca. 2270, 1657, and 1421 BCE, respectively (Fig. 2).

The sedimentary sequence in core S7 is 9 m long, beginning with aeolian sands (9-8.75 m) from the El Abalario Dune Formation (Fig. 2). Holocene greyish ochre clayey silts dominate from 8.75 to the core top. Three sandy layers related to EWEs appear at around 8.5, 5.5, and 2.5 m, being dated at ca. 1983, 1657, and 1142 BCE, respectively (Fig. 2).

4.2. Lithostratigraphy and chronology of the short cores: S6, LB, AR, AA, VT, VAc, VAli.2 and VAli.1

The core S6 recovered 1.5 m of sediments, with clayey silts at the lower part and sands at the upper part (Fig. 2). Sandy facies were dated at 2439 BCE. The core LB is 1.25 m long and it mostly consists of clayey silts. At around 0.9 m, a shelly layer appears with an age of 52 ACE. The sediment record of core AR includes 1.25 m of clayey silts with a shelly layer at around 0.5 m (232 BCE). The core AA has a length of 1.25 m and it is composed of clayey silts with an intercalated shelly layer at around 0.4 m (304 BCE). In the 2-m long core VT, clayey silts range from 2 to 1.25 m, and a thick shelly layer, dated ca. 1304-1151 BCE, occurs towards the top. The core VAc recovered 2 m of sands dated at ca. 1659-1408 BCE. The VAli.2 core (1.75 m long) shows clayey silts in the lower part (1.75-1 m) and a shelly layer (ca. 2205-2022 BCE) in the upper part (1-0 m). The VAli.1 core encompasses 1.4 m of sands dated ca. 2230-2190 BCE.

4.3. Benthic foraminiferal data

The Q-mode principal component analyses (PCA) considering all samples from the studied cores yielded three assemblages (PC-1 to 3), explaining 67.8%, 23.3% and 4.2% of the total variance, respectively (Table 3). The benthic foraminiferal assemblage from the PC-1 is dominated by *Ammonia tepida* with *Haynesina germanica*, *Elphidium translucens* and

Elphidium granosum as secondary species. In the assemblage from the PC-2, *H. germanica* is the unique and dominant species. The assemblage from the PC-3 has *Triloculina trigonula* as dominant species, and includes several additional taxa such as *Ammonia beccarii*, *Quinqueloculina seminula*, *Miliolinella* sp., *Quinqueloculina* sp., *Triloculina* sp., *Quinqueloculina vulgaris*, and *Quinqueloculina laevigata*. All taxa from this assemblage (PC-3) are marine species transported into the estuary by EWEs (Rodríguez-Ramírez et al., 2015). Consequently, they will not be considered to assess the salinity conditions of the Guadalquivir estuary.

The relative abundances of the dominant and secondary taxa from the PC-1 and PC-2 assemblages are shown in Fig. 2. In the S11 core, *H. germanica* shows fairly low values (<20%) from the base to 4.5 m (Fig. 2). Then, it increases until reaching maximal values (80%) from 3 to 2 m, and it decreases upwards. *A. tepida* relative abundance rises from the bottom to 5 m, it diminishes from 5 to 2 m, and it rises towards the core top. *E. translucens* has higher values in the lower part of the core (12.5-5 m), and shows its highest abundance (~25%) at 6.5 m (Fig. 2). In the S7 core, *H. germanica* has very low abundance (<10%) from the core base to 2.5 m, and gradually increasing abundances from 2.5 m towards the core top. *A. tepida* shows considerably high values (40-60%) from the core base to 3.5 m, and it declines upwards. Both *E. translucens* and *E. granosum* have higher abundance (10-35%) from the core bottom to 3.5 m than in the upper part of the core (3.5-1 m), where they virtually disappear. In core S6, both *A. tepida* and *H. germanica* are very abundant (~50%) in interval from 1.25 to 0.75 m, whereas *E. translucens* has very low abundance (<6%) in the same interval. The core LB shows opposite trends for *H. germanica* and *A. tepida*, with higher values of *H. germanica* (~65%) and lower values of *A. tepida* (~25%) from 1.1 to 0.4 m. In the interval from 0.4 to 0.2 m, *A. tepida* increases while *H. germanica* decreases. *E. translucens* and *E. granosum* have very low abundances (<10%) along the core. In the AR and AA cores, *H. germanica* is very abundant

(80-90%), whereas *A. tepida*, *E. translucens* and *E. granosum* show low abundances (<15%) in both cores. The cores VT and VAc have high values of *A. tepida* (50-65%), and low values of *H. germanica* (10-20%). *E. translucens* and *E. granosum* have low values (<15%), decreasing upwards. In the core VAli.2, *A. tepida* shows higher abundances (40-60%), whereas *H. germanica* shows lower abundances (15-30%). Both species abundances drop towards the core top. *E. translucens* and *E. granosum* have very low abundances (<10%). The core VAli.1 has high abundance of *A. tepida* (30-50%), which diminishes upwards. In this core, *H. germanica* and *E. translucens* have very low abundances (<10%).

5. Discussion

5.1. Ecology of benthic foraminiferal species from marginal-marine environments

The two most significant assemblages (PC-1 and PC-2) include *Ammonia tepida*, *Haynesina germanica*, *Elphidium translucens* and *Elphidium granosum* (Table 3). *A. tepida* is a euryhaline species tolerating brackish waters (Murray, 2006; Blázquez and Usera, 2010; Pérez-Asensio and Aguirre, 2010). This species can thrive in environments with low oxygen content and/or high organic matter fluxes (Martins et al., 2013; Wukovits et al., 2018). According to Jorissen et al. (2018), *A. tepida* is a second-order opportunist, which highly increases when organic matter supply is maximal. The species *H. germanica* is also a euryhaline foraminifera resisting a wide range of salinities (Murray, 2006; Blázquez and Usera, 2010). This species can inhabit low oxygenated settings, and it is abundant in sediments with highly variable organic matter content (Alve and Murray, 1999; Martins et al., 2013). *H. germanica* is a third-order opportunist that increases its abundance due to higher organic matter supply, but it is absent when organic matter input is maximal (Jorissen et al., 2018). *E.*

translucens is common in euryhaline marginal-marine environments (Murray, 2006; Pérez-Asensio and Aguirre, 2010). As other *Elphidium* species, it is less tolerant to low oxygen conditions than species from the *Ammonia* group (Sen Gupta and Platon, 2006). This species is an indifferent species, which do not increase with organic matter fluxes, and disappears if organic matter input is high (Jorissen et al., 2018). *E. granosum* is abundant in marginal-marine environments, and tolerates wide salinity changes (euryhaline) (Vaiani, 2000; Curzi et al., 2006; Pérez-Asensio and Aguirre, 2010). This species can benefit from high organic matter fluxes as long as oxygen content is not very low (Jorissen, 1988). It is considered a third-order opportunist, rising its abundance as a response to higher organic matter supply, yet disappearing with maximum organic matter enrichment (Jorissen et al., 2018).

5.2. Development of the Benthic Foraminiferal Salinity index

Benthic foraminiferal assemblages from the Holocene sediments recovered in the Guadalquivir estuary area allowed to developed a new Benthic Foraminiferal Salinity (BFS) index. As mentioned above, the most important species (*A. tepida*, *H. germanica*, *E. translucens*, *E. granosum*) are euryhaline species (i.e., tolerating wide salinity variations). These species can inhabit marginal-marine environments with brackish waters such as estuaries, marshes and littoral lagoons (Debenay, 1995; Ruiz et al., 2005; Murray, 2006; Blázquez and Usera, 2010; Pérez-Asensio and Aguirre, 2010). Marginal-marine environments can have different degrees of salinity related to higher or lower influence of marine waters. This depends on their paleogeography, geomorphology, and wave and tide regimes (Pethick, 1984; Pérez-Ruzafa et al., 2019). The comparison of the Principal Component (PC) scores of species belonging to the euryhaline assemblage PC-1 shows that *A. tepida* and *H. germanica* present higher scores than *E. translucens* and *E. granosum* (Fig. 3, Table 3). This suggests that

higher scores of PC-1 indicate less salinity since *A. tepida* and *H. germanica* have high tolerance to brackish conditions (i.e., less marine influence), and can inhabit inner estuaries (Alve and Murray, 1994; Debenay and Guillou, 2002; Ruiz et al., 2004, 2005; Murray, 2006; Mojtahid et al., 2016). On the contrary, *E. translucens* and *E. granosum*, as other noncarinate elphidiids, occur in outer estuaries with important marine influence (Ruiz et al., 2005; Mojtahid et al., 2016). Considering the environmental conditions indicated by *A. tepida*, *H. germanica*, *E. translucens* and *E. granosum* in the Guadalquivir estuary, a new Benthic Foraminiferal Salinity (BFS) index has been developed for reconstructing salinity changes within overall hyposaline conditions. Consequently, the BFS index was established using the relative abundances of *A. tepida* and *H. germanica* as indicative of lower salinity, and *E. translucens* and *E. granosum* as indicative of higher salinity. The expression of the BFS index is:

BFS index = (% *A. tepida* + *H. germanica*) / (% *A. tepida* + *H. germanica* + *E. translucens* + *E. granosum*)

The BFS index varies from 0 (higher salinity) to 1 (lower salinity), therefore higher values of the index indicate lower salinities, and vice versa. We posit that this BFS index may be a powerful tool to qualitatively reconstruct salinity changes and geomorphological restriction in present-day and ancient marginal-marine environments such as estuaries, marshes and lagoons. Similar indices for reconstructing salinity fluctuations were developed previously (Debenay, 1995; Hayward et al., 2004), but they were based on the relative abundances of a high number of species from benthic foraminiferal assemblages. The calculation of these indices is more complex since it is necessary to perform taxonomic identifications of a high number of species. In contrast, our BFS index requires the identification of a very low number of species, which makes the application of this index easy and rapid. As a result, a profound taxonomic knowledge is not needed to use the index, and a higher number of samples can be analysed more rapidly.

289

290 *5.3. Holocene paleoenvironmental evolution of the Guadalquivir estuary*

291 The Holocene paleoenvironmental evolution of the Guadalquivir estuary was
292 unravelled using the new Benthic Foraminiferal Salinity (BFS) index based on dominant
293 benthic foraminiferal species. In order to assess past paleoenvironmental changes in detail, we
294 use three degrees of salinity based on Debenay (1995) (Fig. 4): 1) higher salinity (BFS index
295 = 0.0-0.4, high marine influence), 2) moderate salinity (BFS index = 0.4-0.7, moderate marine
296 influence), 3) lower salinity (BFS index = 0.7-1.0, low marine influence).

297 In the interval before 2000 BCE, the salinity is higher and moderate in cores at a SW
298 position, near the Atlantic Ocean (cores S7, S11) (Figs 2 and 4). Therefore, this area was well
299 connected with the open sea during this interval. The core S6, located north of cores S7 and
300 S11, records lower salinity, suggesting proximity of paleocoast towards the N. In the eastern
301 area, the cores V.Ali1 and V.Ali2 show high BFS index values (lower salinity) confirming that
302 paleocoast was in a northern position. The morphostratigraphic relationship between V.Ali1,
303 sandy chenier, and V.Ali2, shelly chenier, reflects the progressive restriction of the estuary in
304 the eastern area, before 2000 BCE. These data indicate an overall wide and moderately open
305 paleoestuary, with an efficient connection to the Atlantic Ocean, although the processes of
306 restriction and sedimentary infilling are evident, especially in the east. In this moderately open
307 estuary, marine influence was high as shown by presence of marine fauna transported by tidal
308 flows (Ruiz et al., 2005; Rodríguez-Ramírez et al., 2015).

309 From 2000 to 1400 BCE approximately, the estuary experimented a greater connection
310 with the sea with higher marine influence, principally in distal areas, as a result of subsidence
311 processes, sea-level rise and tsunamis (Rodríguez-Ramírez et al., 2014, 2015). This is
312 especially visible in the nature of sandy sediments, corresponding to a small spit or sandy

chenier, in the upper part of core S6, although without foraminiferal remains, due to intense rework of the sands (Rodríguez-Ramírez et al., 2015). At the SW area (cores S7 and S11), this stronger marine influence is evident by the decrease in BFS index from high to moderate values until 1400 BCE, approximately (Figs 2 and 4). In the eastern area, the lower part of cores VT and VAc show high BFS index values (lower salinity) confirming that the paleocoast was in a more northern position. The absence of sedimentary record at core V.Ali1 might suggest that the NE area was already emerged.

In the interval from 1400 to 1000 BCE, the cores S7 and S11 show increasing BFS index values upwards, and the core S6 could be emerged. This indicates a southward shoreline progradation in the western area. Cores VT and VAc present high BFS index values during the entire interval. The locations of cores V.Ali2 and V.Ali1 were probably emerged. We interpreted the interval from 1400 to 1000 BCE as a phase of estuary restriction leading to a smaller estuary with less connection to the open sea. This interval coincides with the transition from an open estuary to a semiclosed estuary dated at 1200 BCE (Rodríguez-Ramírez et al., 2015). Growth of littoral spits in the river mouth and sedimentary infilling of the estuary may account for this gradual restriction (Rodríguez-Ramírez and Yáñez-Camacho, 2008).

The interval from 1000 BCE to present day is characterised by high BFS index values (lower salinity) in the central area (cores LB, AR, AA) (Figs 2 and 4). In the western area, cores S7 and S11 also show high BFS index values. The location of core S6 was likely emerged during this interval. The eastern area displays high BFS index values in core VT pointing to high geomorphological restriction for the entire interval. In addition, the locations of cores VAc, V.Ali2, and V.Ali1 were surely emerged, suggesting a southward migration of the paleocoast. Therefore, this interval (1000 BCE-present) can be interpreted as a last phase of estuary restriction representing the lowest salinity and highest estuary restriction in the Holocene Guadalquivir estuary evolution.

5.4. Application of the BFS index to other regions

In order to test the applicability of the Benthic Foraminiferal Salinity (BFS) index to other regions, we calculated the index in one sediment core (core 223 S12) and one stratigraphic section (Rambla de la Sepultura (RS) section) from two different regions and environments (Figs 1 and 5): 1) a Pleistocene lagoon in northern Italy (Barbieri and Vaiani, 2018); and 2) a Pliocene coastal bay in southeastern Spain (Pérez-Asensio and Aguirre, 2010). We selected these two regions because, together with the Guadalquivir estuary, they are representative of the most common types of marine-marginal environments. The Pleistocene lagoon from N Italy was a brackish lagoon environment (Barbieri and Vaiani, 2018). Benthic foraminiferal assemblages from lagoonal sediments from core 223 S12 were dominated by *Ammonia parkinsoniana* and intermediate *Ammonia tepida–Ammonia parkinsoniana* forms, with secondary taxa including *Haynesina germanica*, *Aubignyna perlucida*, *Ammonia tepida*, and *Cribroelphidium granosum* (Barbieri and Vaiani, 2018). The Pliocene coastal bay from SE Spain was a restricted coastal bay with coral banks, which was filled with terrigenous sediments of prograding fan deltas (Pérez-Asensio and Aguirre, 2010). In the RS section from this sheltered bay, benthic foraminiferal assemblages were mainly characterised by species from the genus *Ammonia* (*A. beccarii*, *A. tepida*, *A. inflata*) and noncarinate *Elphidium* species (*E. translucens*, *E. granosum*) (Pérez-Asensio and Aguirre, 2010). BFS index values from these different locations and environments were compared with the BFS index values from core S7 (Fig. 5). In this core from the Holocene Guadalquivir estuary, BFS index increased from low to high values in the lower part of the core, indicating progressive restriction. The BFS index values decreased in the middle part of the core, indicating better connection to the Atlantic Ocean. Finally, values increased from moderate to high values, marking the final phase of estuary restriction. In the core 223 S12 from the Pleistocene lagoon of northern Italy, BFS

index was overall high along the core, except for two samples at 163.2 and 161.9 m (Fig. 5). These values suggest that this marginal-marine environment was highly restricted, and only experienced better connection to the sea episodically. This interpretation is consistent with a brackish lagoon environment with minor environmental fluctuations related to both freshwater and marine water inputs (Barbieri and Vaiani, 2018). The BFS index values from the Pliocene coastal bay from southeastern Spain increased gradually from low to high values along the RS section. This upward decrease in salinity is in good agreement with a brackish environment that was progressively restricted due to the progradation of fan deltas (Pérez-Asensio and Aguirre, 2010).

After applying the BFS index to two other regions, we propose that our index can be successfully applied to different regions, environments and timescales. This is very feasible because the four species used to calculate the index are widespread in marginal-marine environments around the world. To calculate the index, it is only necessary the presence of *A. tepida* or *H. germanica*, and *E. translucens* or *E. granosum*. Additionally, if *E. translucens* and *E. granosum* are not found, other noncarinate elphidiids with similar ecological requirements might be used (e.g. *Cribroelphidium excavatum*) (Mojtahid et al., 2016). Accordingly, only two to four species are needed to be identified, making the application of the index to other regions simple and fast.

6. Conclusions

Benthic foraminiferal distribution and abundance from the Holocene Guadalquivir estuary are controlled by the degree of salinity. This relationship allowed us to develop a simple Benthic Foraminiferal Salinity (BFS) index based on four benthic foraminiferal species (*A. tepida*, *H. germanica*, *E. translucens*, *E. granosum*). Since the BFS index is based on the

identification of a very low species number, it is easy to calculate, even for scientists lacking a profound knowledge on benthic foraminiferal taxonomy. The low number of species to be identified also permits to calculate the BFS index rapidly, which is a great advantage for large-scale studies involving a high number of samples and sites.

The BFS index has allowed us to describe reliably the Holocene paleoenvironmental evolution of the Guadalquivir estuary with great detail, validating the index as proxy for different degrees of salinity, and therefore marine influence. We used three degrees of salinity (higher = 0.0-0.4, moderate = 0.4-0.7, lower = 0.7-1.0), which help us to differentiate subtle changes in geomorphological restriction during the Holocene. According to the BFS index values, the Holocene paleoenvironmental evolution of the estuary had four distinct phases: 1) wide and moderately open estuary (> 2000 BCE), with high connection to the Atlantic Ocean allowing the entrance of transported marine fauna; 2) (2000-1400 BCE) expansion of estuary due to sea-level rise and subsidence; 3) a phase of estuary restriction (1400-1000 BCE), with southward shoreline progradation related to spits growth and sedimentary infilling, which coincides with the transition from open to semiclosed estuary; 4) last phase of estuary restriction (1000 BCE-present day), with the lowest salinity and highest estuary restriction.

Our BFS index can also be applied to other regions, environments and timescales, identifying only two to four species (*A. tepida* or *H. germanica* + *E. translucens* or *E. granosum*). This means the index is simple and rapid to calculate, and useful for qualitatively reconstructing salinity changes in worldwide marginal-marine environments from different time periods.

Declaration of competing interest

The authors state that they have no competing financial or personal interests that could represent a conflict of interest.

411

412 **Acknowledgments**

413 We are very grateful to the Editor-in-Chief, Professor Thomas J. Algeo, for his
414 comments and the editorial handling of this manuscript. We also would like to thank two
415 anonymous reviewers for their very constructive comments, which greatly improved this
416 manuscript. We thank the Fundación Caja de Madrid, Fundación Doñana 21, Ayuntamiento de
417 Hinojos, Fundación FUHEM, Estación Biológica de Doñana (EBD), Espacio Natural de
418 Doñana (END), Instituto Andaluz del Patrimonio Histórico (IAPH), Delegación de Cultura of
419 Junta de Andalucía in Huelva, and Organismo Autónomo Parques Nacionales of Ministerio de
420 Medio Ambiente y Medio Rural y Marino for their support of the Hinojos Project. Additional
421 support by Junta de Andalucía to the Research Groups RNM-276 and RNM-190 is also
422 acknowledged. JNPA is member of the Research Groups RNM-190 (Junta de Andalucía), GRC
423 Geociències Marines (2017 SGR 315, Generalitat de Catalunya), and Climate Research Group
424 (CEREGE).

425

426 **References**

427 Alve, E., Murray, J.W., 1994. Ecology and taphonomy of benthic foraminifera in a temperate
428 mesotidal inlet. J. Foramin. Res. 24, 18–27. http://dx.doi.org/10.2113/gsjfr.24.1.18.
429 Alve, E., Murray, J.W., 1999. Marginal marine environments of the Skagerrak and Kattegat: a
430 baseline study of living (stained) benthic foraminiferal ecology. Palaeogeogr.
431 Palaeoclimatol. Palaeoecol. 146, 171–193. https://doi.org/10.1016/S0031-
432 0182(98)00131-X

Barbieri, G., Vaiani, S.C., 2018. Benthic foraminifera or Ostracoda? Comparing the accuracy of palaeoenvironmental indicators from a Pleistocene lagoon of the Romagna coastal plain (Italy). J. Micropalaeontol. 37, 203–230. https://doi.org/10.5194/jm-37-203-2018

Blázquez, A.M., Usera, J., 2010. Palaeoenvironments and Quaternary foraminifera in the Elx coastal lagoon (Alicante, Spain). Quat. Int. 221, 68–90. https://doi.org/10.1016/j.quaint.2009.06.033

Blázquez, A.M., Rodríguez-Pérez, A., Torres, T., Ortiz, J.E., 2017. Evidence for Holocene sea level and climate change from Almenara marsh (western Mediterranean). Quat. Res. 88, 206–222. https://doi.org/10.1017/qua.2017.47

Blázquez-Morilla, A.M., Rodríguez-Pérez, A., Sanjuán-Lamata, D., 2019. Palaeoenvironmental evolution from the early Holocene to the present of the Almenara marsh (western Mediterranean). Sci. Mar. 82, 257–268. https://doi.org/10.3989/scimar.04853.07A

Chiverrell, R.C., 2001. A proxy record of late Holocene climate change from May Moss, northeast England. J. Quaternary Sci. 16, 9–29. https://doi.org/10.1002/1099-1417(200101)16:1<9::AID-JQS568>3.0.CO;2-K

Curzi, P.V., Dinelli, E., Ricci Lucchi, M., Vaiani, S.C., 2006. Palaeoenvironmental control on sediment composition and provenance in the late Quaternary deltaic successions: a case study from the Po delta area (Northern Italy). Geological Journal 41, 591–612. https://doi.org/10.1002/gj.1060

Debenay, J.-P., 1995. Can the confinement index (calculated on the basis of foraminiferal populations) be used in the study of coastal evolution during the quaternary? Quat. Int. 29–30, 89–93. https://doi.org/10.1016/1040-6182(95)00001-Y

456 Debenay, J.-P., Guillou, J.-J., 2002. Ecological transitions indicated by foraminiferal
457 assemblages in paralic environments. Estuaries 25, 1107–1120.
458 http://dx.doi.org/10.1007/BF02692208
459 Debenay, J.-P., Luan, B.T., 2006. Foraminiferal assemblages and the confinement index
460 as tools for assessment of saline intrusion and human impact in the Mekong Delta
461 and neighbouring areas (Vietnam). Rev. Micropaleontol. 49, 74–85.
462 https://doi.org/10.1016/j.revmic.2006.01.002
463 Debenay, J.-P., Bicchi, E., Goubert, E., Armynot du Châtelet, E., 2006. Spatio-temporal
464 distribution of benthic foraminifera in relation to estuarine dynamics (Vie estuary,
465 Vendée, W France). Estuar. Coast. Shelf Sci. 67, 181–197.
466 https://doi.org/10.1016/j.ecss.2005.11.014
467 Devillers, B., Bony, G., Degeai, J.-P., Gascò, J., Lachenal, T., Bruneton, H., Yung, F., Oueslati,
468 H., Thierry, A., 2019. Holocene coastal environmental changes and human occupation
469 of the lower Hérault River, southern France. Quat. Sci. Rev. 222, 105912.
470 https://doi.org/10.1016/j.quascirev.2019.105912
471 Di Bella, L., Casieri, S., Carboni, M.G., 2008. Late Quaternary paleoenvironmental
472 reconstruction of the Tremiti structural high (Central Adriatic Sea) from benthic
473 foraminiferal assemblages. Geobios 41, 729–742.
474 https://doi.org/10.1016/j.geobios.2008.06.001
475 Durand, M., Mojtahid, M., Maillet, G.M., Proust, J.-N., Lehay, D., Ehrhold, A., Barré, A.,
476 Howa, H., 2016. Mid- to late-Holocene environmental evolution of the Loire estuary as
477 observed from sedimentary characteristics and benthic foraminiferal assemblages. J.
478 Sea Res. 118, 17–34. https://doi.org/10.1016/j.seares.2016.08.003
479 Gerdes, G., Petzelberger, B.E.M., Scholz-Böttcher, B.M., Streif, H., 2003. The record of
480 climatic change in the geological archives of shallow marine, coastal, and adjacent

lowland areas of Northern Germany. Quat. Sci. Rev. 22, 101–124. https://doi.org/10.1016/S0277-3791(02)00183-X

Gregoire, G., Le Roy, P., Ehrhold, A., Jouet, G., Garlan, T., 2017. Control factors of Holocene sedimentary infilling in a semi-closed tidal estuarine-like system: the bay of Brest (France). Mar. Geol. 385, 84–100. https://doi.org/10.1016/j.margeo.2016.11.005

Guelorget, O., Perthuisot, J.P., 1983. Le domaine paralique. Expressions géologiques, biologiques et économiques du confinement. Trav. Lab. Gdol. ENS Paris, 16, 1–136.

Guelorget, O., Perthuisot, J.P., 1992. The Paralic Realm. Biological organization and functioning. Vie Milieu 42, 215–251.

Haas, T. de, Valk, L. van der, Cohen, K.M., Pierik, H.J., Weisscher, S.A.H., Hijma, M.P., Spek, A.J.F. van der, Kleinhans, M.G., 2019. Long-term evolution of the Old Rhine estuary: Unravelling effects of changing boundary conditions and inherited landscape. Depositional Rec. 5, 84–108. https://doi.org/10.1002/dep2.56

Hayward, B.W., Scott, G.H., Grenfell, H.R., Carter, R., Lipps, J.H., 2004. Techniques for estimation of tidal elevation and confinement (~salinity) histories of sheltered harbours and estuaries using benthic foraminifera: examples from New Zealand. Holocene 14, 218–232. https://doi.org/10.1191/0959683604hl678rp

Jiménez-Moreno, G., Rodríguez-Ramírez, A., Pérez-Asensio, J.N., Carrión, J.S., López-Sáez, J.A., Villarías-Robles, J.J., Celestino-Pérez, S., Cerrillo-Cuenca, E., León, Á., Contreras, C., 2015. Impact of late-Holocene aridification trend, climate variability and geodynamic control on the environment from a coastal area in SW Spain. Holocene 25, 607–617. https://doi.org/10.1177/0959683614565955

Jorissen, F.J., 1988. Benthic foraminifera from the Adriatic Sea; principles of phenotypic variation. Utrecht Micropaleontology Bulletin 37, 1–176.

505 Jorissen, F.J., Fontanier, C., Ellen, T., 2007. Paleoceanographical proxies based on deep-sea
506 benthic foraminiferal assemblage characteristics. In: Hillaire-Marcel, C., De Vernal,
507 A. (Eds.), Developments in Marine Geology, Vol. 1. Elsevier, Amsterdam, pp. 263–
508 325.

509 Jorissen, F.J., Nardelli, M.P., Almogi-Labin, A., Barras, C., Bergamin, L., Bicchi, E., El Kateb,
510 A., Ferraro, L., McGann, M., Morigi, C., Romano, E., Sabbatini, A., Schweizer, M.,
511 Spezzaferri, S., 2018. Developing Foram-AMBI for biomonitoring in the
512 Mediterranean: species assignments to ecological categories. Mar. Micropaleontol.
513 140, 33–45. https://doi.org/10.1016/j.marmicro.2017.12.006.

514 Loeblich Jr., A.R., Tappan, H., 1987. Foraminiferal Genera and Their Classification. 2
515 Volumes. 1: 970 pp.; 2: 213 pp. 847 pls. Van Reinhold Company, New York.

516 Martins, V.A., Frontalini, F., Tramonte, K.M., Figueira, R.C.L., Miranda, P., Sequeira, C., et
517 al., 2013. Assessment of the health quality of Ria de Aveiro (Portugal): Heavy metals
518 and benthic foraminifera. Mar. Pollut. Bull. 70, 18–33.
519 https://doi.org/10.1016/j.marpolbul.2013.02.003

520 Martins, V.A., Frontalini, F., Rodrigues, M.A., Dias, J.M.A., Laut, L.L.M., Silva, F.S.,
521 Clemente, I.M.M.M., Reno, R., Moreno, J., Sousa, S.M.S., Zaaboub, N., El Bour, M.,
522 Rocha F., 2014. Foraminiferal Biotopes and their Distribution Control in Ria de Aveiro
523 (Portugal): a multiproxy approach. Environ. Monit. Assess. 186, 8875–8897.
524 https://doi.org/10.1007/s10661-014-4052-7

525 Milker, Y., Schmiedl, G., Betzler, C., Römer, M., Jaramillo-Vogel, D., Siccha, M., 2009.
526 Distribution of recent benthic foraminifera in shelf carbonate environments of the
527 Western Mediterranean Sea. Mar. Micropaleontol. 73, 207–225.
528 https://doi.org/10.1016/j.marmicro.2009.10.003

529 Milker, Y, Schmiedl, G, 2012. A taxonomic guide to modern benthic shelf foraminifera of the
530 western Mediterranean Sea. Palaeontol. Electron. 15, 16A, 134 p. palaeo-
531 electronica.org/content/2012-issue-2-articles/223-taxonomyforaminifera.

532 Mojtahid, M., Geslin, E., Coynel, A., Gorse, L., Vella, C., Davranche, A., Zozzolo, L.,
533 Blanchet, L., Bénéteau, E., Maillet, G., 2016. Spatial distribution of living (Rose Bengal
534 stained) benthic foraminifera in the Loire estuary (western France). J. Sea Res. 118, 1–
535 16. https://doi.org/10.1016/j.seares.2016.02.003

536 Murray, J.W., 2006. Ecology and Applications of Benthic Foraminifera. Cambridge University
537 Press, Cambridge, 426 pp.

538 Parker, W.C., Arnold, A.J., 1999. Quantitative methods of analysis in foraminiferal ecology.
539 In: Sen Gupta, B.K. (Ed.), Modern Foraminifera. Kluwer Academic Publishers,
540 Dordrecht, pp. 71–89.

541 Pérez-Asensio, J.N., Aguirre, J., 2010. Benthic foraminiferal assemblages in temperate coral-
542 bearing deposits from the late Pliocene. J. Foramin. Res. 40, 61–78.
543 https://doi.org/10.2113/gsjfr.40.1.61

544 Pérez-Asensio, J.N., Aguirre, J., Schmiedl, G., Civis, J., 2012. Messinian paleoenvironmental
545 evolution in the lower Guadalquivir Basin (SW Spain) based on benthic foraminifera.
546 Palaeogeogr. Palaeoclimatol. Palaeoecol. 326–328, 135–151

547 Pérez-Asensio, J.N., Aguirre, J., Schmiedl, G., Civis, J., 2014. Messinian productivity changes
548 in the northeastern Atlantic and their relationship to the closure of the Atlantic–
549 Mediterranean gateway: implications for Neogene palaeoclimate and
550 palaeoceanography. J. Geol. Soc. London 171, 389–400.
551 https://doi.org/10.1144/jgs2013-032

Pérez- Asensio, J.N., Aguirre, J., Rodríguez- Tovar, F.J., 2017. The effect of bioturbation by polychaetes (Opheliidae) on benthic foraminiferal assemblages and test preservation. Palaeontology 60, 807–827. https://doi.org/10.1111/pala.12317

Pérez-Asensio, J.N., Frigola, J., Pena, L.D., Sierro, F.J., Reguera, M.I., Rodríguez-Tovar, F.J., Dorador, J., Asioli, A., Kuhlmann, J., Huhn, K., Cacho, I., 2020. Changes in western Mediterranean thermohaline circulation in association with a deglacial Organic Rich Layer formation in the Alboran Sea. Quat. Sci. Rev. 228, 106075. https://doi.org/10.1016/j.quascirev.2019.106075

Pérez-Ruzafa, A., De Pascalis, F., Ghezzo, M., Quispe-Becerra, J.I., Hernández-García, R., Muñoz, I., Vergara, C., Pérez-Ruzafa, I.M., Umgiesser, G., Marcos, C., 2019. Connectivity between coastal lagoons and sea: Asymmetrical effects on assemblages' and populations' structure. Estuar. Coast. Shelf Sci. 216, 171-186. https://doi.org/10.1016/j.ecss.2018.02.031

Pethick, J., 1984. An Introduction to Coastal Geomorphology. Hodder Arnold Publication, 257 pp.

Reimer, P.J., Bard, E., Bayliss, A., Beck, J.W., Blackwell, P.G., Ramsey, C.B., Buck, C.E., Cheng, H., Edwards, R.L., Friedrich, M., Grootes, P.M., Guilderson, T.P., Haflidason, H., Hajdas, I., Hatté, C., Heaton, T.J., Hoffmann, D.L., Hogg, A.G., Hughen, K.A., Kaiser, K.F., Kromer, B., Manning, S.W., Niu, M., Reimer, R.W., Richards, D.A., Scott, E.M., Southon, J.R., Staff, R.A., Turney, C.S.M., Plicht, J. van der, 2013. IntCal13 and Marine13 Radiocarbon Age Calibration Curves 0–50,000 Years cal BP. Radiocarbon 55, 1869–1887. https://doi.org/10.2458/azu_js_rc.55.16947

Rich, V.I., Maier, R.M., 2015. Chapter 6 - Aquatic Environments, in: Pepper, I.L., Gerba, C.P., Gentry, T.J. (Eds.), Environmental Microbiology (Third Edition). Academic Press, San Diego, pp. 111–138. https://doi.org/10.1016/B978-0-12-394626-3.00006-5

577 Rodríguez-Ramírez, A., Yáñez-Camacho, C.M., 2008. Formation of chenier plain of the
578 Doñana marshland (SW Spain): Observations and geomorphic model. Mar. Geol. 254,
579 187–196. https://doi.org/10.1016/j.margeo.2008.06.006
580 Rodríguez-Ramírez, A., Ruiz, F., Cáceres, L.M., Rodríguez Vidal, J., Pino, R., Muñoz, J.M.,
581 2003. Analysis of the recent storm record in the southwestern Spanish coast:
582 implications for littoral management. Sci. Total Environ. 303, 189–201.
583 https://doi.org/10.1016/S0048-9697(02)00400-X
584 Rodríguez-Ramírez, A., Flores-Hurtado, E., Contreras, C., Villarías-Robles, J.J.R., Jiménez-
585 Moreno, G., Pérez-Asensio, J.N., López-Sáez, J.A., Celestino-Pérez, S., Cerrillo-
586 Cuenca, E., León, Á., 2014. The role of neo-tectonics in the sedimentary infilling and
587 geomorphological evolution of the Guadalquivir estuary (Gulf of Cadiz, SW Spain)
588 during the Holocene. Geomorphology 219, 126–140.
589 https://doi.org/10.1016/j.geomorph.2014.05.004
590 Rodríguez-Ramírez, A., Pérez-Asensio, J.N., Santos, A., Jiménez-Moreno, G., Villarías-
591 Robles, J.J.R., Mayoral, E., Celestino-Pérez, S., Cerrillo-Cuenca, E., López-Sáez, J.A.,
592 León, Á., Contreras, C., 2015. Atlantic extreme wave events during the last four
593 millennia in the Guadalquivir estuary, SW Spain. Quat. Res. 83, 24–40.
594 https://doi.org/10.1016/j.yqres.2014.08.005
595 Rodríguez-Ramírez, A., Villarías-Robles, J.J.R., Pérez-Asensio, J.N., Santos, A., Morales,
596 J.A., Celestino-Pérez, S., León, Á., Santos-Arévalo, F.J., 2016. Geomorphological
597 record of extreme wave events during Roman times in the Guadalquivir estuary (Gulf
598 of Cadiz, SW Spain): An archaeological and paleogeographical approach.
599 Geomorphology 261, 103–118. https://doi.org/10.1016/j.geomorph.2016.02.030

600 Rodríguez-Ramírez, A., Villarías-Robles, J.J.R., Pérez-Asensio, J.N., Celestino-Pérez, S.
601 2019, The Guadalquivir Estuary: Spits and Marshes. In: Morales, J.A. (Ed.), The
602 Spanish Coastal Systems. Springer, Switzerland, pp. 517–541.

603 Ruiz, F., González-Regalado, M.L., Borrego, J., Abad, M., Pendón, J.G., 2004. Ostracoda and
604 foraminifera as short-term tracers of environmental changes in very polluted areas: the
605 Odiel Estuary (SW Spain). Environ. Pollut. 129, 49–61.
606 https://doi.org/10.1016/j.envpol.2003.09.024

607 Ruiz, F., González-Regalado, M.L., Pendón, J.G., Abad, M., Olías, M., Muñoz, J.M., 2005.
608 Correlation between foraminifera and sedimentary environments in recent estuaries of
609 Southwestern Spain: Applications to holocene reconstructions. Quat. Int. 140–141, 21–
610 36. https://doi.org/10.1016/j.quaint.2005.05.002

611 Sen Gupta, B.K., Platon, E., 2006. Tracking past sedimentary records of oxygen depletion in
612 coastal waters: USE of the *Ammonia–Elphidium* foraminiferal index. Journal of Coastal
613 Research Special 39, 1331–1355.

614 Shepard F.P., 1954. Nomenclature based on sand-silt-clay ratios. Journal of Sedimentary
615 Petrology 24, 151–158. https://doi.org/10.1306/D4269774-2B26-11D7-
616 8648000102C1865D

617 Soares, A.M., 2015. Datación radiocarbónica de conchas marinas en el golfo de Cádiz: El
618 efecto reservorio marino, su variabilidad durante el Holoceno e inferencias
619 paleoambientales. Cuaternario y geomorfología 29, 19–29.

620 Spanish Ministry of Fomento, 2005. Información climática de nivel del mar. Mareógrafo de
621 Sevilla (Bonanza), 6 pp.

622 Stuiver, M., Reimer, P.J., 1993. Extended ^{14}C Data Base and Revised CALIB 3.0 ^{14}C Age
623 Calibration Program. Radiocarbon 35, 215–230.
624 https://doi.org/10.1017/S0033822200013904

625 Vaiani, S.C., 2000. Testing the applicability of strontium isotope stratigraphy in marine to
626 deltaic Pleistocene deposits: An example from the Lamone River Valley (Northern
627 Italy). J. Geol. 108, 585–599. https://doi.org/10.1086/314416
628 Vanney, J.R., 1970. L'hydrologie du Bas Guadalquivir. CSIC, Departamento de Geografía
629 Aplicada, Madrid.
630 Wukovits, J., Oberrauch, M., Enge, A.J., Heinz, P., 2018. The distinct roles of two intertidal
631 foraminiferal species in phytodetrital carbon and nitrogen fluxes—Results from
632 laboratory feeding experiments. Biogeosciences 15, 6185–6198.
633 https://doi.org/10.5194/bg-15-6185-2018
634 Ybert, J.-P., Bissa, W.M., Catharino, E.L.M., Kutner, M., 2003. Environmental and sea-level
635 variations on the southeastern Brazilian coast during the Late Holocene with comments
636 on prehistoric human occupation. Palaeogeogr. Palaeoclimatol. Palaeoecol. 189, 11–
637 24. https://doi.org/10.1016/S0031-0182(02)00590-4
638

639 **Figure captions**

640 **Figure 1.** Study area and location of the short and deep cores. The Spanish local term ‘caño’
641 refers to a relict, fully filled-in tidal-fluvial channel. Upper map created with GeoMapApp
642 (http://www.geomapapp.org/). (For interpretation of the references to colour in this figure
643 legend, the reader is referred to the Web version of this article).

644

645 **Figure 2.** Lithostratigraphy, chronology and benthic foraminiferal data (dominant species %,
646 BFS index) of the short and deep cores. (For interpretation of the references to colour in this
647 figure legend, the reader is referred to the Web version of this article).

648

Figure 3. Principal Component (PC) scores of the dominant euryhaline benthic foraminiferal species of the short and deep cores. (For interpretation of the references to colour in this figure legend, the reader is referred to the Web version of this article).

Figure 4. Benthic foraminiferal Salinity index values (BFS index) of the short and deep cores showing the Holocene paleoenvironmental evolution of the Guadalquivir estuary. (For interpretation of the references to colour in this figure legend, the reader is referred to the Web version of this article).

Figure 5. Comparison of the Benthic Foraminiferal Salinity index values (BFS index) of three marginal-marine environments from different regions and timescales: core S7 (this study), core 223 S12 (Barbieri and Vaiani, 2018), and Rambla de la Sepultura (RS) section (Pérez-Asensio and Aguirre, 2010) (For interpretation of the references to colour in this figure legend, the reader is referred to the Web version of this article).

Table captions

Table 1. Location (latitude, longitude) of the studied short and long cores (S6, LB, AR, AA, VT, VAc, VAli.2 VAli.1, S7, S11).

Table 2. Radiocarbon ^{14}C data using the CALIB 7.10 software (Stuiver and Reimer, 1993), the calibration dataset of Reimer et al. (2013), and a ΔR value of -108 ± 31 ^{14}C yr (Soares, 2015). Uncertainties of the calibrated ages are expressed as 2σ errors. B.—Beta Analytic Laboratory (Miami, USA). CNA.—Centro Nacional de Aceleradores (Seville, Spain). DAMS.—Accium

672 BioSciences Accelerator Mass Spectrometry Lab (Seattle, USA). CX.—Geochron
673 Laboratories, Krueger Enterprises, Inc. (Cambridge, USA). (1) Rodríguez-Ramírez et al.
674 (2014). (2) Rodríguez-Ramírez et al. (2015). (3) Rodríguez-Ramírez et al. (2016).

675

676 **Table 3.** Q-mode principal component analysis results from the short and deep cores.
677 Explained variance (%) of each PC axis (assemblage), and the dominant and secondary species
678 are indicated.

679

680 **Supplementary material**

681 The supplementary material file contains the raw and processed benthic foraminiferal
682 data from the short and deep cores including raw counts, relative abundances (%) of dominant
683 species, and BFS index values. This file also includes the BFS index values used in Figure 5.

Figure 1

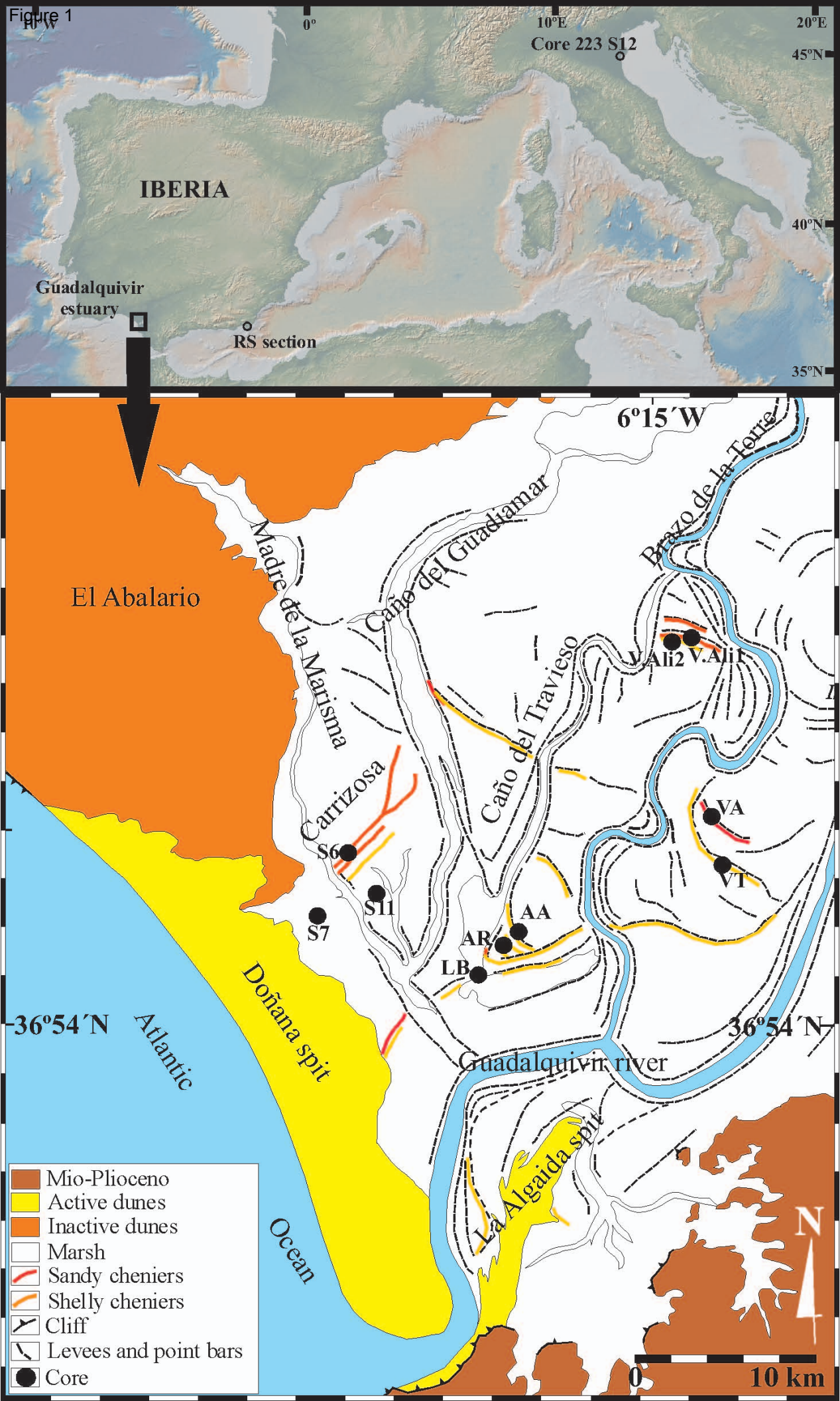
0°
10°E
20°E
Core 223 S12
45°N
IBERIA
40°N
Guadalquivir estuary
RS section
35°N
6°15´W
El Abalario
Madre de la Marisma
Caño del Guadiamar
Brazo de la Torre
V.Ali2
V.Ali1
Caño del Travieso
Carrizosa
VA
VT
S6
S11
S7
AA
AR
LB
36°54´N
Doñana spit
Atlantic
Guadalquivir river
La Algaida spit
Ocean
Mio-Plioceno
Active dunes
Inactive dunes
Marsh
Sandy cheniers
Shelly cheniers
Cliff
Levees and point bars
Core
N
0
10 km

Figure 2

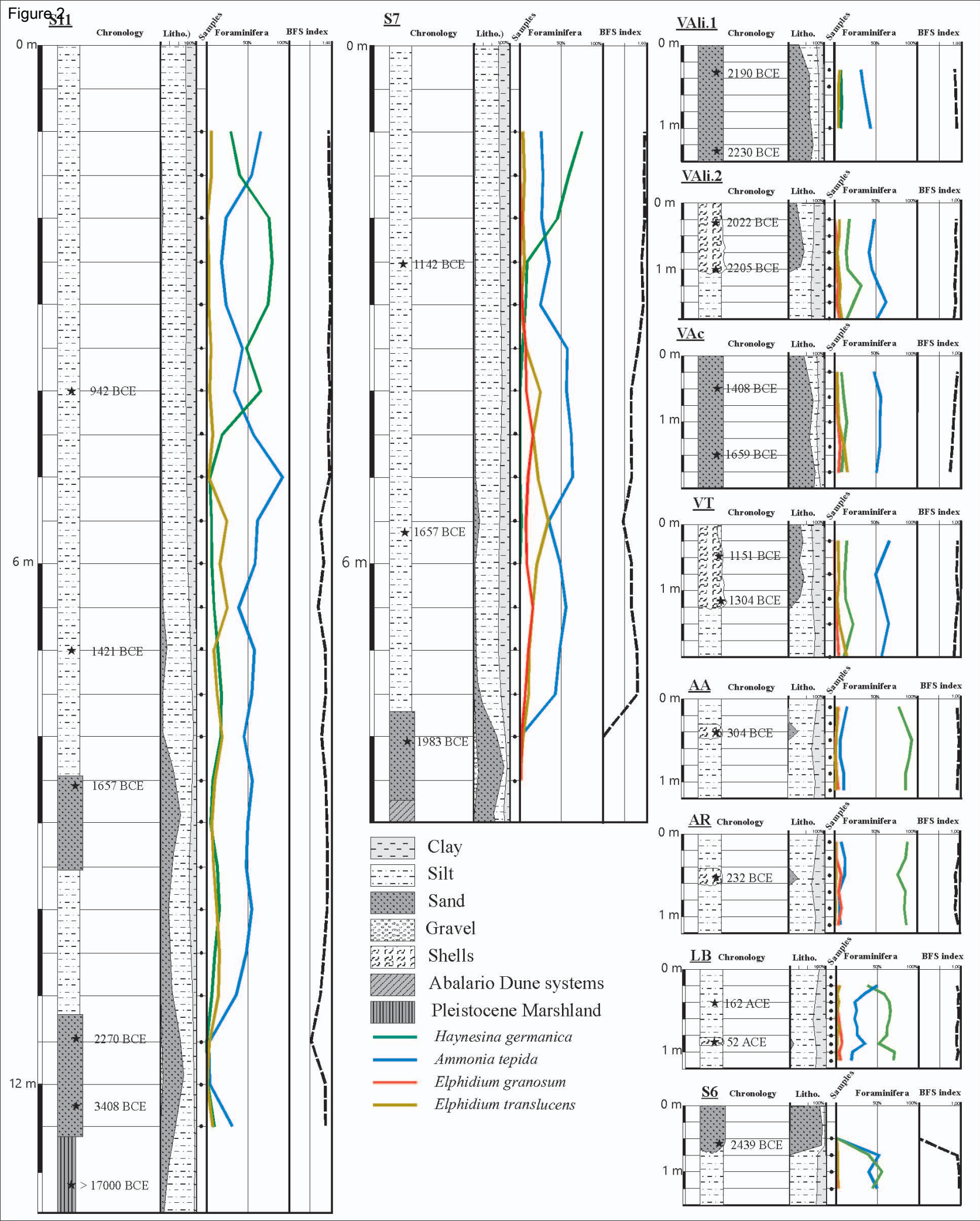
S11
Chronology
Litho.)
Samples
Foraminifera
BFS index
0 m
6 m
12 m
942 BCE
1421 BCE
1657 BCE
2270 BCE
3408 BCE
> 17000 BCE
S7
1142 BCE
1657 BCE
1983 BCE
Clay
Silt
Sand
Gravel
Shells
Abalario Dune systems
Pleistocene Marshland
Haynesina germanica
Ammonia tepida
Elphidium granosum
Elphidium translucens
VAli.1
2190 BCE
2230 BCE
VAli.2
2022 BCE
2205 BCE
VAc
1408 BCE
1659 BCE
VT
1151 BCE
1304 BCE
AA
304 BCE
AR
232 BCE
LB
162 ACE
52 ACE
S6
2439 BCE
1 m

Figure 3

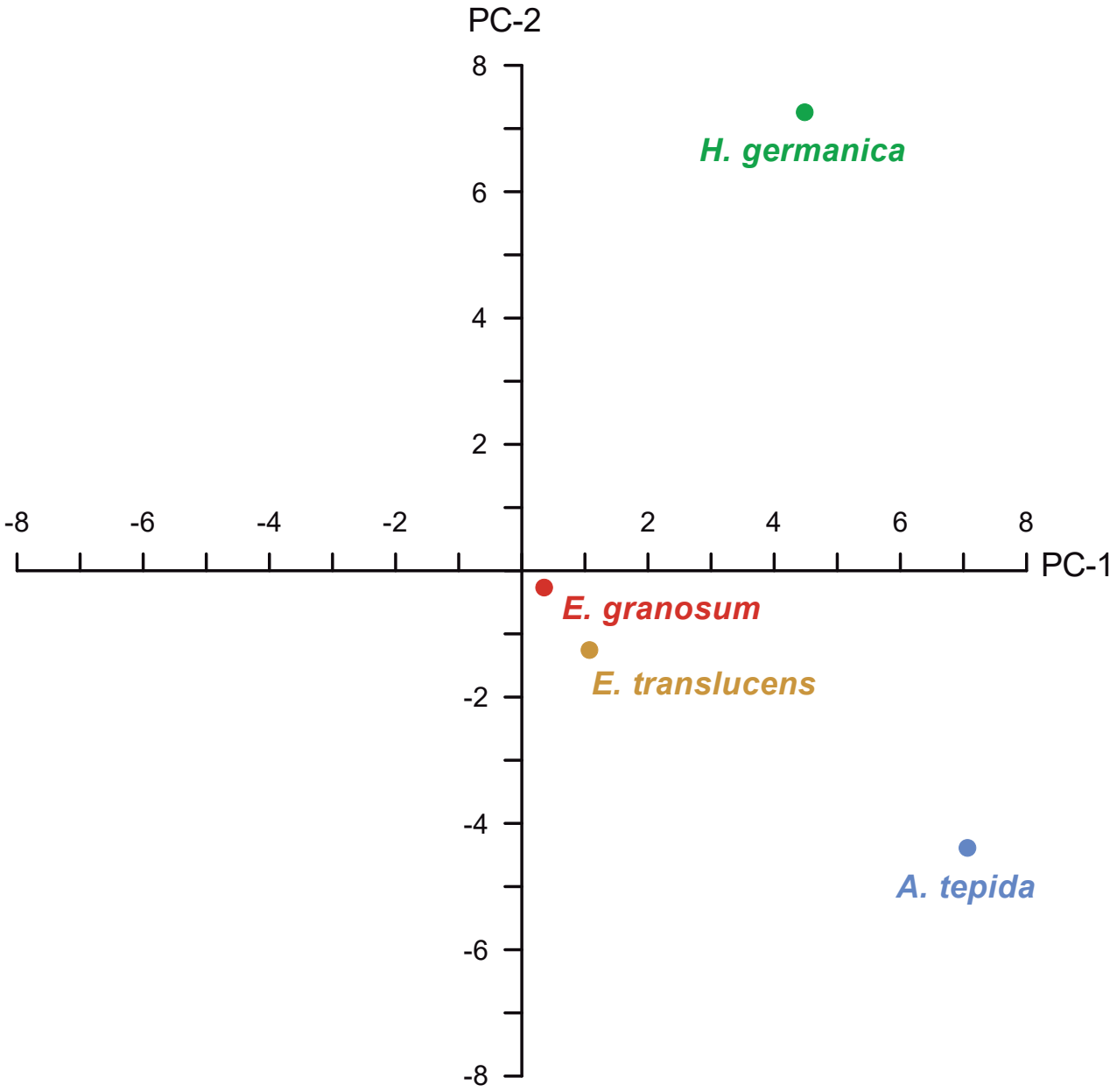
PC-2
8
6
4
2
-2
-4
-6
-8
-8
-6
-4
-2
2
4
6
8
PC-1
H. germanica
E. granosum
E. translucens
A. tepida

Figure 4

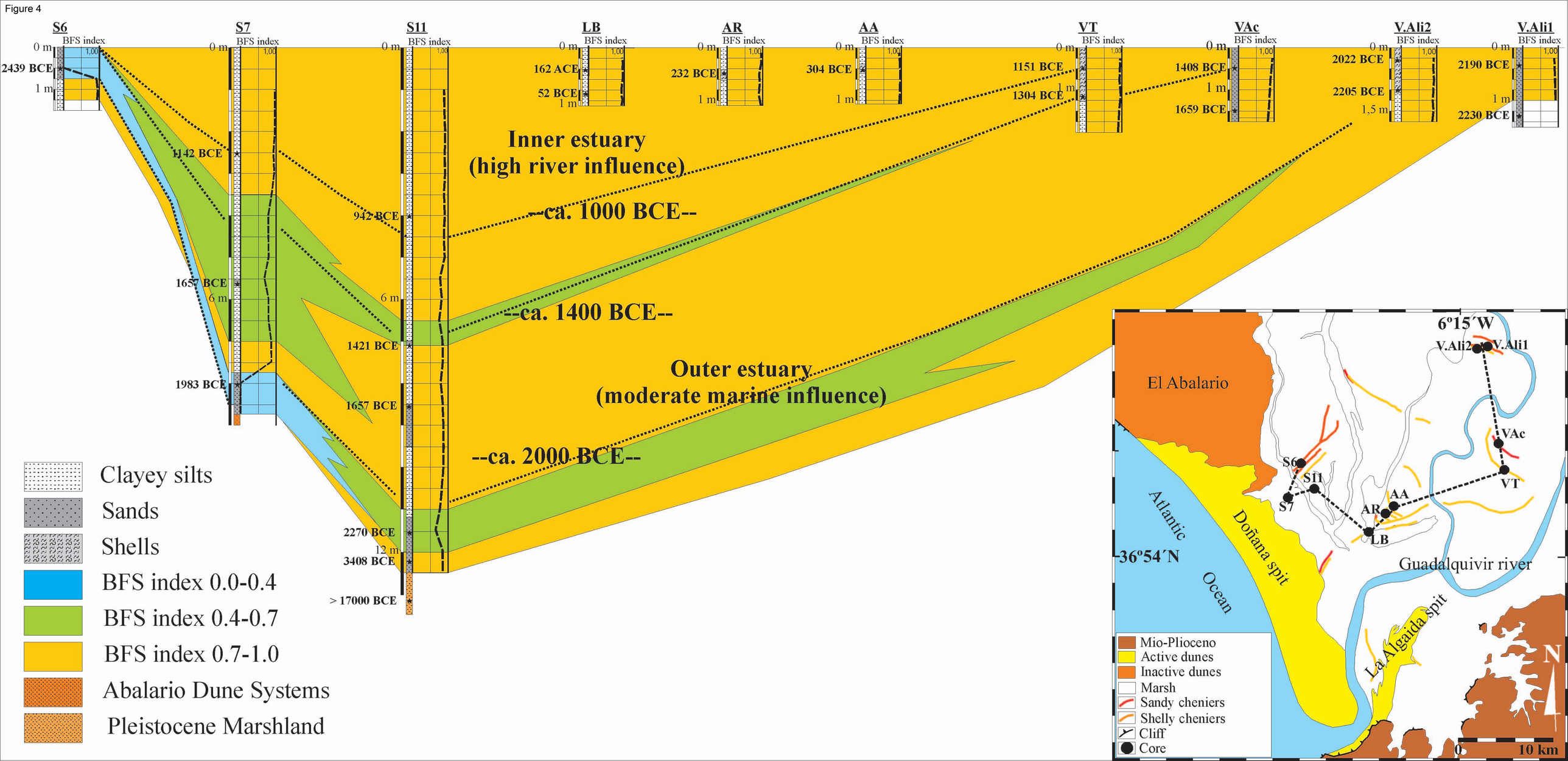
S6
S7
S11
LB
AR
AA
VT
VAc
V.Ali2
V.Ali1
BFS index
0 m
1 m
6 m
12 m
2439 BCE
142 BCE
1657 BCE
1983 BCE
942 BCE
1421 BCE
1657 BCE
2270 BCE
3408 BCE
> 17000 BCE
162 ACE
52 BCE
232 BCE
304 BCE
1151 BCE
1304 BCE
1408 BCE
1659 BCE
2022 BCE
2205 BCE
1,5 m
2190 BCE
2230 BCE
Inner estuary
(high river influence)
--ca. 1000 BCE--
--ca. 1400 BCE--
Outer estuary
(moderate marine influence)
--ca. 2000 BCE--
Clayey silts
Sands
Shells
BFS index 0.0-0.4
BFS index 0.4-0.7
BFS index 0.7-1.0
Abalario Dune Systems
Pleistocene Marshland
6º15´W
36º54´N
El Abalario
Atlantic
Ocean
Doñana spit
La Algaida spit
Guadalquivir river
Mio-Plioceno
Active dunes
Inactive dunes
Marsh
Sandy cheniers
Shelly cheniers
Cliff
Core
N
0
10 km

2-5 pt
Figure 5